OPEN

Metallic Artifact Reduction of Multiacquisition With Variable Resonance Image Combination Selective–Short Tau Inversion Recovery for Postoperative Cervical Spine With Artificial Disk Replacement: A Preliminary Study

Jeong Kyeom Kim, MD, Yeo Ju Kim, MD,† Seunghun Lee, MD,† Daehyun Yoon, PhD,‡ Ro Woon Lee, MD,* Jung Ui Hong, MD,* Dal-Sung Ryu, MD,§ and Jiyoon Bae, MD||*

Objective: This study aimed to evaluate multiacquisition with variable resonance image combination selective short tau inversion recovery (MAVRIC SL STIR) for metallic artifact reduction in magnetic resonance imaging (MRI) of postoperative cervical spine with artificial disk replacement.

Methods: A porcine cervical spine with artificial disk replacement was subject to 3 T MRI with variable fat-suppressed fluid-sensitive sequences. Five volunteers underwent MRI with MAVRIC SL STIR and STIR. Quantitative and qualitative analyses were performed for metallic artifact reduction.

Results: MAVRIC SL STIR showed the least signal void areas in the tissue phantom and volunteer study. In the tissue phantom study, MAVRIC SL STIR showed the best visualization of anatomic structure, least distortion, and signal pile-up. However, it ranked last for the homogeneity of fat suppression among sequences. In the volunteer study, MAVRIC SL STIR showed better visualization of anatomic structure and lesser distortion, but showed worse image quality of the spinal cord than STIR in the sagittal plane ($P < 0.05$).

Conclusions: MAVRIC SL STIR might be useful for visualization of anatomy by reduction of signal void areas and distortion in the operated site but should be used as a complement to STIR for evaluation of the spinal cord signal change.

Key Words: MAVRIC SL STIR, metallic artifact, artificial disk replacement, cervical spine, fat suppression

(*J Comput Assist Tomogr* 2022;46: 274–281)

From the *Department of Radiology, College of Medicine, Inha University, Jung-gu, Incheon; †Department of Radiology, Hanyang University School of Medicine, Seoul Hospital, Seoul, Korea; ‡Department of Radiology, Stanford University, Stanford, CA; §Department of Neurosurgery, College of Medicine, Inha University, Jung-gu, Incheon; and ||Department of Pathology, National Police Hospital, Seoul, South Korea.

Received for publication May 27, 2021; accepted September 1, 2021.

Correspondence to: Yeo Ju Kim, MD, PhD, Department of Radiology, Hanyang University School of Medicine, Seoul Hospital, 222-1 Wangsimni-ro, Seongdong-gu, Seoul 04763, South Korea (e-mail: kimyeoju@hanyang.ac.kr).

This work was supported by a National Research Foundation of Korea grant funded by the Korea government (Ministry of Science and ICT; No.2017R1C1B5017781).

The authors declare no conflict of interest.

Author contribution: Conceptualization: Y.J.K., R.W.L.; Data curation: J.K.K., J.U.H., D.-S.R.; Formal analysis: Y.J.K., S.L.; Funding acquisition: Y.J.K.; Resources: J.K.K., J.U.H., R.W.L.; Writing—original draft: Y.J.K. D.Y.; Writing—review & editing: J.B.

DOI: 10.1097/RCT.0000000000001266

Artificial disk replacement (ADR) after discectomy for cervical spine has the potential to become a widespread technique for the treatment of cervical degenerative disk disease.[1,2] The clinical outcomes of ADR are similar to those of anterior cervical discectomy and fusion (ACDF) but with less loss of segment motion and risk of adjacent level degeneration.[3] However, postoperative magnetic resonance imaging (MRI) in ADR cases has great limitation in visualization of the operated site and adjacent neural structure because of metallic artifacts regardless of the metal property, compared with ACDF.[4–6] This is related to the fact that the anteroposterior dimension of the artificial disk for the cover of the end plate is longer than cages, which are used at the ACDF, and a location closer to the spinal cord.[4–6]

In postoperative MRI, the fat-suppressed fluid-sensitive technique might be the key sequence because it can sensitively detect edema or fluid containing pathologic tissue in the neural structure, bone marrow, and around the disk implant by suppressing bright adipose signals.[7–9] However, it also suffers from off-resonance artifact around metal, including signal loss, distortion, signal pile-up, and incomplete fat suppression.[8,9] In clinical practice, short tau inversion recovery (STIR) and Dixon-based techniques may allow relatively homogeneous fat suppression around metals compared with spectral fat saturation.[10,11] Multiacquisition with variable resonance image combination (MAVRIC) and slice-encoding metal artifact correction have been developed for metal artifact reduction.[12,13] Multiacquisition with variable resonance image combination selective (MAVRIC SL) has the advantages of both techniques by retaining the slab selectivity (Z-selectivity) of slice-encoding metal artifact correction by way of a Z gradient and by retaining the higher SNR of MAVRIC by an overlapped spectral strategy with multiple frequency-selective excitation.[14] Multiacquisition with variable resonance image combination selective has been shown to successfully reduce metallic artifacts in the knee, hip, and extremities.[15,16] However, to the best of our knowledge, MAVRIC SL STIR has not been evaluated for postoperative cervical spine with ADR. The purpose of our study was to evaluate MAVRIC SL STIR for metallic artifact reduction in MRI of postoperative cervical spine with ADR.

METHODS

General Electric (GE) Healthcare (Waukesha, Wisconsin) provided research support for the implantation and application of MAVRIC SL. This study was prospectively designed and approved by the institutional review board of our hospital. Informed consent was obtained from all participating volunteers. This study comprised a tissue phantom study using porcine cervical spine with variable fat-suppressed fluid-sensitive sequences and a volunteer study using STIR and MAVRIC SL STIR.

TABLE 1. MRI Protocol of Tissue Phantom Study

	Axial					Sagittal				
	2D				3D	2D				3D
	T2 FS	Flex T2	IDEAL T2	STIR	MAVRIC SL STIR	T2 FS	Flex T2	IDEAL T2	STIR	MAVRIC SL STIR
TR, ms	4423	3796	3858	7296	2400	3100	2500	2500	4727	2265.9
TE, ms	91.8	90.5	92	65	15.6	88.3	85.4	88.3	27.3	14.2
FA, °	142	142	142	142	75	142	142	142	142	75
ETL	18	28	17	19	48	20	12	12	14	48
NEX	3	4	6	3	2	4	4	6	2	2
BW, kHz	50	83.3	83.3	41.67	125	50	83.3	83.3	41.67	125
Matrix size	320 × 224	320 × 224	320 × 224	320 × 224	320 × 256	320 × 256	352 × 224	352 × 224	320 × 224	320 × 224
ST/gap, mm	3/0	3/0	3/0	3/0	3/0	3/0	3/0	3/0	3/0	3/0
FOV, mm	180 × 180	180 × 180	180 × 180	180 × 180	180 × 180	240 × 240	240 × 240	240 × 240	240 × 240	240 × 240
TI, ms				200	200				200	200
Frequency encoding direction	AP	AP	AP	AP	AP	AP	AP	AP	AP	AP
Scan time, min	3:10	2:10	3:12	2:50	9:32	3:05	3:38	4:18	3:17	10:43

Number of spectral bins of MAVRIC SL STIR = 18.

BW indicates bandwidth; FA, flip angle; NEX, number of excitations; TI, inversion time.

Tissue Phantom Study

Tissue Preparation and MRI Scan

A fresh porcine cervical spine including posterior cervical soft tissue was obtained within 24 hours of death. A neurosurgeon inserted a cervical artificial disk (ProDisc, Implant M, width of 15 mm, depth of 12 mm; DePuy Synthes, West Chester, Pennsylvania) via the standard right anterior approach at the intervertebral disk space between the third (C3) and fourth cervical vertebra (C4). Like other artificial disk instruments, the Prodisc-C is a ball-and-socket mechanism with metal end plates embedded into the bone with cobalt chrome keels.[7] After the operation, the porcine cervical spine was placed in a plastic container filled with water and scanned in a 3-T MR system (Architect; GE) with a head and neck coil. The MRI protocol included axial and sagittal T2-weighted fast spin-echo (FSE) sequence with spectral fat saturation (T2 FS), with 2-point Dixon fat/water separation (Flex T2), and with iterative decomposition of water and fat with echo asymmetry and least-squares estimation (IDEAL T2), STIR, and MAVRIC SL STIR (Table 1). In particular, for MAVRIC SL STIR, a calibration scan was obtained to enable the scanner to automatically determine the spectral frequency cutoff specific to the implant being imaged and, in turn, to determine the number of spectral bins, which was 18 in this tissue phantom study. The imaging parameters for the calibration scan were as follows: repetition time (TR)/echo time (TE), 2433.2/10; receive bandwidth, ±125 kHz; field of view (FOV), 40 cm; acquisition matrix, 128 × 32; section thickness (ST), 6 mm; echo train length (ETL), 16; and scan time, approximately 1 minute and 57 seconds.

TABLE 2. Demographic Data of Volunteers

	Volunteer 1	Volunteer 2	Volunteer 3	Volunteer 4	Volunteer 5
Sex	Male	Male	Male	Female	Male
Age, y	51	39	32	45	48
Preoperative diagnosis	Herniated disk	Herniated disk	Herniated disk	Herniated disk	Herniated disk
Operated level	C5–6	C4–5	C5–6	C5–6	C5–6
Postoperative period, y	9	6	4	6	6
Postoperative symptom	None	None	None	None	None

TABLE 3. MRI Protocol of the Volunteer Study

	Axial		Sagittal	
	STIR (2D)	MAVRIC SL STIR (3D)	STIR (2D)	MAVRIC SL STIR (3D)
TR, ms	2936	3963	5948	3746
TE, ms	70	60	70	60
FA, °	142	115	142	115
ETL	14	20	14	20
NEX	2	1	2	1
BW, kHz	41.67	125	41.67	125
Matrix size	320 × 224	320 × 192	320 × 224	320 × 192
ST/gap, mm	3/0	3/0	3/0	3/0
FOV, mm	140	180	240	240
TI	200	200	200	200
Frequency encoding direction	AP	AP	AP	AP
Scan time	1:40	9:21	3:16	10: 42

The automatically determined number of spectral bins was variable per volunteer, between 14 and 20.

BW, bandwidth; FA, flip angle; NEX, number of excitations; TI = inversion time.

TABLE 4. Scoring System According to Each Category of the Qualitative Analysis of the Volunteer Study

Visualization of the anatomic structure (axial and sagittal plane)	1: Less than 25% of anatomic structure being visible 2: 25% to 50% of anatomic structure being visible 3: 50% to 75% of anatomic structure being visible 4: More than 75% being visible 5: Clear image without any artifacts
Image quality of the spinal cord (axial and sagittal plane)	1: Severe blurring and noise with no clinical use 2: Moderate blurring and noise resulting in limited clinical use 3: Mild blurring and noise 4: Clear image without blurring and noise
Distortion (sagittal plane)	1: Severe distortion made the anatomic allocation of the implant impossible 2: Distortion moderately impaired anatomic allocation near the metal implant 3: Distortion mildly altered anatomic contour 4: No distortion present
Pileup (sagittal plane)	1: Severe pileup with obliteration of normal anatomy or signal 2: Moderate pileup with partial obliteration of normal anatomic structure or signal 3: Mild pileup without significant effect on normal anatomic structure or signal 4: No pileup
Fat suppression (sagittal plane)	1: Failure of fat suppression >75% of FOV 2: Failure of fat suppression about 50%–75% of FOV 3: Failure of fat suppression about 25%–50% of FOV 4: Failure of fat suppression <25% of FOV

Imaging Analysis

Quantitative Study

A senior radiology resident measured the area of signal loss around the prosthesis in all axial and sagittal sequences of the tissue phantom study using the Maroview PACS system (Maroview 5.4; Infinite, Seoul, South Korea) under the supervision of a musculoskeletal radiologist.

Qualitative Study

Four continuous axial images of the midportion of the prosthesis were selected for the axial image set. Two continuous midsagittal images for spinal cord and one each parasagittal image for the right and left pedicular levels were selected for the sagittal image set. The image data sets were newly labeled, instead of sequence names, for blinding the sequence. Two musculoskeletal radiologists with 10 and 14 years of experience independently evaluated the image data sets. Each newly labeled sequence was ranked from 1 to 5 for the visualization of the anatomic structure as follows: the anterior subarachnoid space, spinal cord, both neural foramina and anterior paravertebral soft tissue for the axial and sagittal planes, and apposing upper and lower vertebral bodies at the operated site in the sagittal plane. They assigned 1 for best visualization of the anatomic structure and 5 for the worst. They also evaluated the distortion, signal pileup, and homogeneity of fat suppression and ranked them in the axial and sagittal planes. Distortion was defined as changed or impaired anatomic allocation around the prosthesis. Signal pile-up was defined as the peripheral rim of high signal intensity around the prosthesis. Least artifact was assigned 1 and most 5.

Volunteer Study

Volunteer Enrollment and MRI Scan

The demographic data are shown in Table 2. All volunteers performed sagittal STIR and MAVRIC SL STIR sequences, and 3 of them performed axial STIR and Mavric SL STIR sequences

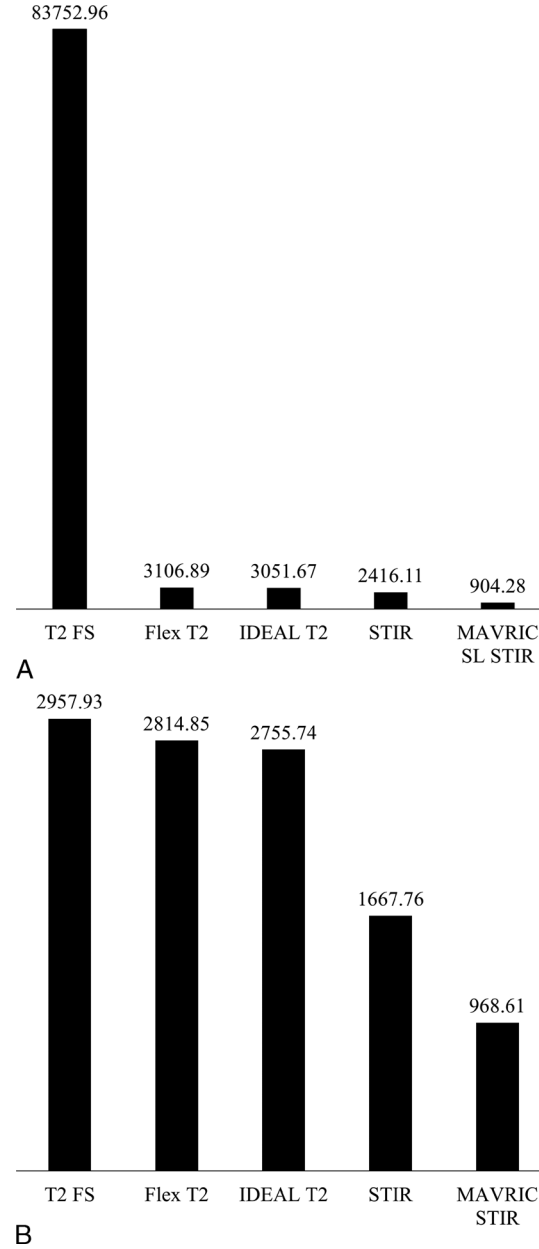

FIGURE 1. Result of the sum of areas (in millimeters squared) of signal void of each sequence in axial (A) and sagittal planes (B) of the tissue phantom study. Sum of areas of signal void of each sequence is noted at the top of corresponding bar.

TABLE 5. Average Rank of Each Sequence for Visualization of the Anatomic Structure

	Sagittal						Axial			
Rank	**AS**	**SC**	**NF**	**PV**	**UVB**	**LVB**	**AS**	**SC**	**NF**	**PV**
1	MAVRIC SL STIR	MAVRIC SL STIR	MAVRIC SL STIR	MAVRIC SL STIR	MAVRIC SL STIR	MAVRIC SL STIR	MAVRIC SL STIR	MAVRIC SL STIR	MAVRIC SL STIR	MAVRIC SL STIR
2	STIR	STIR	STIR	STIR	STIR	STIR	STIR	STIR	STIR	STIR
3	IDEAL T2	Flex T2	Flex T2	IDEAL T2	T2 FS	T2FS	IDEAL T2	IDEAL T2	IDEAL T2	IDEAL T2
4	Flex T2	IDEAL T2	IDEAL T2	Flex T2	Flex T2	Flex T2	Flex T2	Flex T2	Flex T2	Flex T2
5	T2FS	T2 FS	T2 FS	T2 FS	IDEAL T2	IDEAL T2	T2FS	T2FS	T2FS	T2FS

Each sequence was ranked from 1 to 5 for the visualization of the anatomic structure: 1 for best visualization of the anatomic structure and 5 for the worst.

AS indicates anterior subarachnoid space; LVB, lower vertebral body; NF, both neural foramina; PV, anterior paravertebral soft tissue; SC, spinal cord; UVB, upper vertebral body.

additionally. Scan coverage was the whole cervical bony structures in the sagittal plane, but only at the operated level in the axial plane. Before MAVRIC SL STIR, a calibration scan was also obtained in the same manner as in the tissue phantom study. The automatically determined number of spectral bins was variable per volunteer, between 14 and 20. The detail MRI protocol is shown in Table 3.

Image Analysis

Quantitative study

A senior radiology resident measured the area of signal loss around the prosthesis in the sagittal plane in the same manner as in the tissue phantom study under the supervision of a musculoskeletal radiologist.

Qualitative study

After the MRI scan, the axial and sagittal image data sets from each sequence were also relabeled as in the tissue phantom study to remove the original sequence name and the information.

Two musculoskeletal radiologists who evaluated the tissue phantom study independently assessed images using the following categories: visualization of anatomic structure, image quality of the spinal cord, distortion, signal pile-up, and homogeneity of fat suppression. The visualization of the anatomic structure was assessed for the same structures as in the tissue phantom study in the axial and sagittal planes using a 5-point scale scoring system (Table 4). The right and left neural foramen was separately scored then averaged. Image quality of the spinal cord was assessed in the axial and sagittal planes. The distortion, signal pile-up, and fat

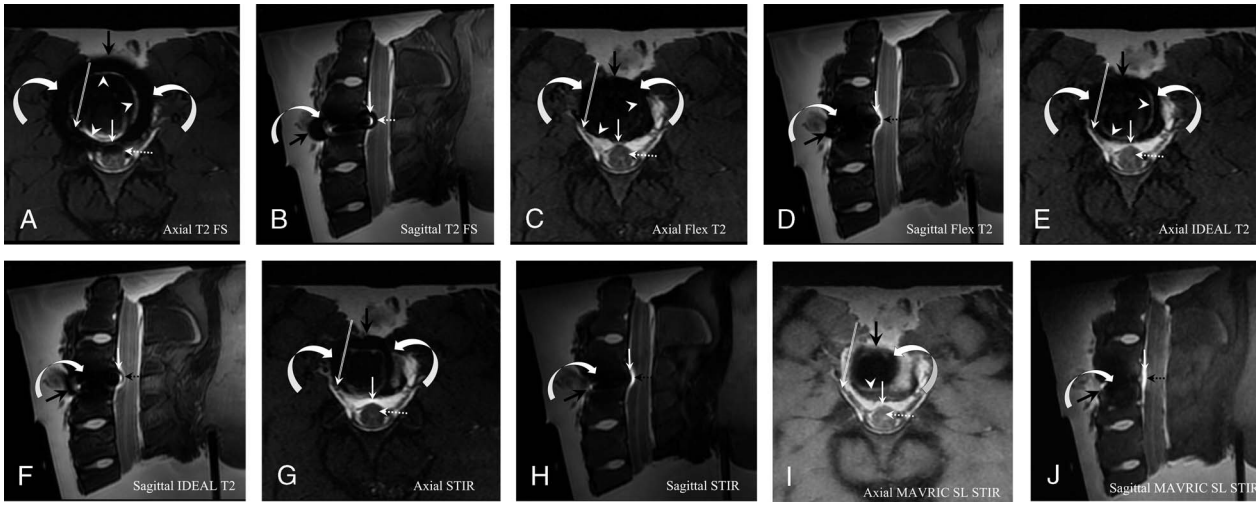

FIGURE 2. Axial images of variable fat-suppressed fluid-sensitive sequence of postoperative porcine cervical spine with ADR. A and B, Axial (A) and sagittal (B) images of T2 FS show a large area of signal void (curved arrows in A and B) with intense signal pile-up (arrowheads in A). By signal void, the anterior subarachnoid space (arrow in A and B), anterior portion of the spinal cord (dashed arrow in A and B), right neutral foramen (double-lined arrow in A), and anterior paravertebral soft tissue (black arrow in A and B) are obscured. C–F, Axial and sagittal images of Flex T2 (C and D) and IDEAL T2 (E and F) show lesser signal void area (curved arrows in C–F) and weaker signal pile-up (arrowheads in C and E) than that of T2 FS (A and B). The spinal cord is clearly visualized in the axial images (dashed arrow in C and E). In the sagittal images, there is a distortion (black dashed arrow in D and F) that can be mistaken for indentation of the spinal cord near artificial disk. Note the partial obliteration of the anterior subarachnoid space (arrow in C–F), right neutral foramen (double-lined arrow in C and E), and anterior paravertebral soft tissue (black arrow in C–F) by signal void. G and H, In axial (G) and sagittal (H) image of STIR, the signal void area (curved arrow in G and H) is further reduced compared with those of T2 FS (A and B), Flex T2 (C and D), and IDEAL T2 (E and F). The anterior subarachnoid space (arrow in G and H), neutral foramen (double-dashed arrow in G), and anterior paravertebral soft tissue (black arrow in G and H) were minimally obliterated by signal void. Note the mild distortion (dashed black arrow in H) at the spinal cord. I and J, Axial (I) and sagittal (J) image of MAVRIC SL STIR showed the least area of signal void (curved arrows in I and J) and signal pile-up (arrowheads in I), and best for the depiction of subarachnoid space (arrow in I and J), spinal cord (dashed arrow in I), right neutral foramen (double-lined arrow in I), and anterior paravertebral soft tissue (black arrow in I and J). Note the almost absence of the distortion (black dashed arrow in J) of the spinal cord.

TABLE 6. Average Rank of Each Sequence for the Distortion, Pileup, and Homogeneity of Fat Suppression

	Sagittal			Axial		
Rank	**Distortion**	**Signal Pileup**	**Fat Suppression**	**Distortion**	**Signal Pileup**	**Fat Suppression**
1	MAVRIC SL STIR	MAVRIC SL STIR	STIR IDEAL T2 Flex T2	MAVRIC SL STIR	MAVRIC SL STIR	STIR IDEAL T2 Flex T2
2	STIR	IDEAL T2		STIR	IDEAL T2	
3	IDEAL T2	Flex T2		IDEAL T2 Flex T2	Flex T2	
4	Flex T2	STIR T2	T2 FS MAVRIC SL STIR		STIR	T2 FS MAVRIC SL STIR
5	T2FS	T2 FS		T2 FS	T2 FS	

Each sequence was ranked from 1 to 5 for the distortion, signal pile-up, and fat suppression. The least distortion, signal pile-up, and the best homogeneity fat suppression were assigned 1, and the most distortion, signal pile-up, and the worst homogeneity of fat suppression were assigned 5.

suppression were evaluated in the sagittal plane. The scoring system according to each category is shown in Table 4.

Statistical Analysis

Weighted Cohen κ statistic (κ value) was calculated to determine the interobserver agreement of the tissue phantom study and volunteer study. The strength of agreement quantified by a κ statistic was graded as follows: <0, poor; 0.01 to 0.20, slight; 0.21 to 0.40, fair; 0.41 to 0.60, moderate; 0.61 to 0.80, substantial; and 0.81 to 0.99, almost perfect.

For the tissue phantom study, the sum of areas of signal void was also calculated for each sequence. The average rank of each sequence between 2 readers was calculated for the depiction of anatomic structure, distortion, signal pile-up, and homogeneity of fat suppression in the axial and sagittal planes. In the volunteer study, the sum of areas of signal void for each sequence in the sagittal plane was compared using Wilcoxon signed rank test. For each evaluation category of qualitative study, the scores from 2 readers were averaged and also compared between the sequences using Wilcoxon signed rank test.

All statistical analyses were performed using statistical software (MedCalc, version 10.4.0.0, MedCalc Software, SPSS 21; SPSS Inc, Chicago, Illinois). Statistical significance was set at $P < 0.05$ for all tests of significance.

RESULTS

Tissue Phantom Study

Quantitative study

MAVRIC SL STIR showed the least signal void areas followed by STIR, in both the axial and sagittal planes (Fig. 1).

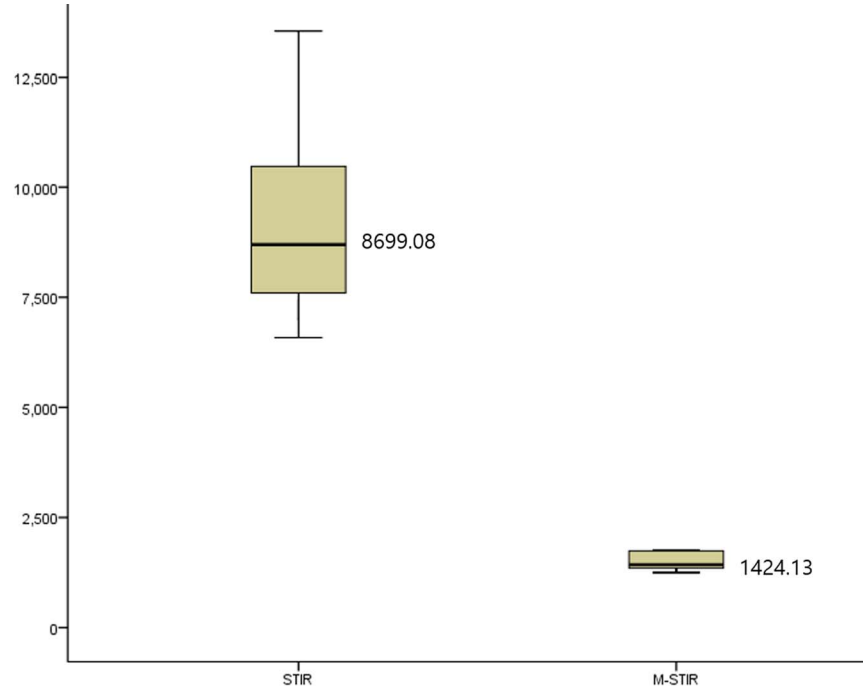

FIGURE 3. Results of the sum of areas (in millimeters squared) of signal void of STIR and MAVRIC STIR in the sagittal plane of the volunteer study. Numbers on the right side of the box are the median values of the sum of areas of signal void of the five volunteers ($P = 0.043$). Figure 3 can be viewed online in color at www.jcat.org.

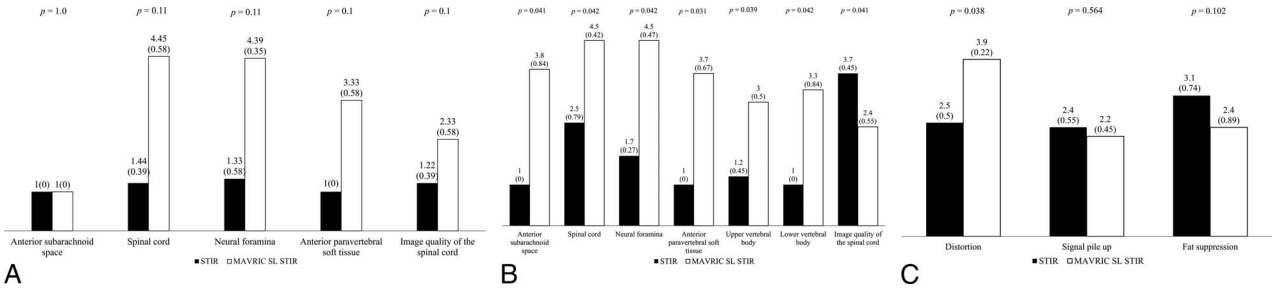

FIGURE 4. Results of qualitative analysis in the volunteer study. Numbers on the top of the bar are the average score, and numbers in parentheses are the standard deviation of the 5 volunteers. *P* value of each category was noted at the top of the graph. A, Average scores of the depiction of anatomic structure and image quality of the spinal cord of the STIR and MAVRIC SL STIR in the axial plane. B, Average scores of the depiction of anatomic structure and image quality of the spinal cord of the STIR and MAVRIC SL STIR in the sagittal plane. C, Average scores of the distortion, signal pile-up, and fat suppression of the STIR and MAVRIC SL STIR in the sagittal plane.

Qualitative study

The interobserver agreement of the rank of sequences between the 2 readers was substantial ($\kappa = 0.7$) for the whole qualitative analysis.

For visualization of the anatomic structure, MAVRIC SL STIR showed the best results, followed by STIR, in the axial and sagittal planes (Table 5, Fig. 2). In the axial and sagittal planes, MAVRIC SL STIR showed the least distortion and signal pile-up but ranked last for the homogeneity of fat suppression (Table 6, Fig. 2). STIR showed most homogeneous fat suppression and second rank for the distortion in axial and sagittal planes.

Volunteer Study

Quantitative Study

There were statistically significant differences among the areas of signal void of each sequence in the sagittal plane ($P = 0.043$). The median value of signal void area of STIR was more than 6 times larger than that of MAVRIC SL STIR (Fig. 3).

Qualitative study

The interobserver agreement of the whole qualitative analysis between the 2 readers was almost perfect ($\kappa = 0.89$).

The average scores of the depiction of the anatomy of MAVRIC SL STIR in the sagittal plane were higher than those of STIR for all anatomical structures with statistical significance (Fig. 4, $P < 0.05$). In the axial plane, MAVRIC SL STIR was also scored higher than STIR for the depiction of the spinal cord, neutral foramina, and anterior paravertebral soft tissue, although there was no statistical significance (Fig. 4, $P > 0.05$). Especially for the spinal cord and neural foramina, MAVRIC SL STIR documented an average score of more than 4 points, which meant almost complete visualization in both the axial and sagittal planes (Figs. 4–6).

In terms of the image quality of the spinal cord, MAVRIC SL STIR had moderate noise with limited clinical use. In the sagittal plane, STIR showed better image quality than MAVRIC SL STIR with statistical significance ($P = 0.041$; Figs. 4, 6). In the axial plane, MAVRIC SL STIR had slightly better image quality than STIR without statistical significance ($P > 0.05$; Figs. 4, 5).

The distortion showed statistically significant differences between the sequences ($P = 0.029$; Figs. 4, 6). The MAVRIC SL STIR showed almost no distortion. However, the signal pile-up artifact did not show statistically significant differences ($P = 0.564$; Fig. 4). The pattern of signal pile-up artifact of MAVRIC SL STIR was an ill-defined, mild, high signal adjacent to the metal, which was different from that of STIR, which showed a peripheral intense bright high signal. Although the high signal of signal pile-up in MAVRIC SL STIR was not intense, it overlapped with the spinal cord and apposed vertebral bodies, mimicking pathology (Figs. 6, 7). The homogeneity of fat suppression did

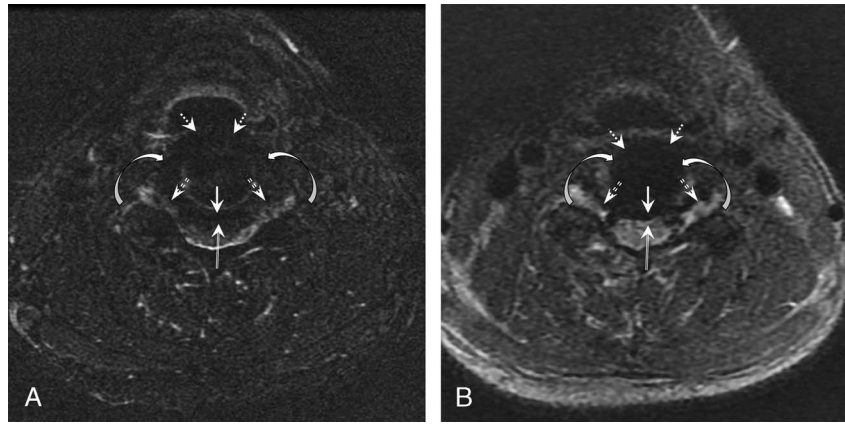

FIGURE 5. Axial MR images of the operated level of a 39-year-old man with ADR at C4–C5 (volunteer 2). A, STIR image shows obliteration of the anterior subarachnoid space (arrow) and anterior paravertebral soft tissue (dashed arrows) by signal void (curved arrows). Partly obliteration of the spinal cord (double-lined arrow) and both neural foramina (double dashed arrows) near the artificial disk. Moderate blurring and noise are seen in the spinal cord. B, MAVRIC SL STIR image shows an obliterated anterior subarachnoid space by signal void (dashed arrow) and flow artifact. However, the spinal cord, both neural foramina, and anterior paravertebral soft tissue around the artificial disk are well visualized despite mild to moderate blurring and noise.

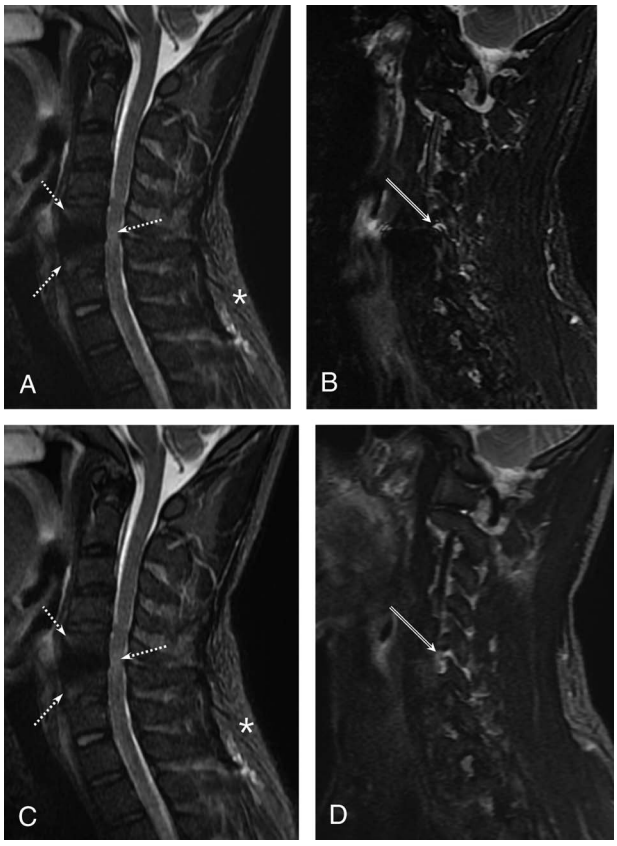

FIGURE 6. Sagittal MR images of the cervical spine of a 51-year-old man with ADR at C5–C6 (volunteer 1). A, Midsagittal image of STIR shows near obliteration of the anterior subarachnoid space and anterior paravertebral soft tissue. The spinal cord is visualized only at its posterior half at the operated level. The image of the spinal cord exhibits mild blurring and noise. Distortion (arrows) and signal pile-up (dashed arrows) are also seen around the operated site. B, In the parasagittal image of STIR, only the superior portion of the neural foramen (double arrow) is visible because of metallic artifact. C, Midsagittal image of MAVRIC SL STIR partly visualizes the anterior subarachnoid space and the anterior paravertebral soft tissue. The spinal cord is almost completely visualized at the operated level. The image of the spinal cord exhibits mild blurring and noise. Distortion is almost absent. However, ill-defined, mild high signal intensities (dashed arrows) are seen at the bone marrow and spinal cord around the operated site, suggesting pile-up artifact. These high signal intensities exist adjacent to the metal. Note the insufficient fat suppression at the posterior portion of the neck (asterisk). D, Parasagittal image of MAVRIC SL STIR almost completely visualizes the neural foramen (double arrow).

not show a statistically significant difference ($P = 0.102$; Fig. 4), although MAVRIC SL STIR presented less homogeneous fat suppression than STIR.

DISCUSSION

We compared MAVRIC SL STIR with other conventional fat-suppressed fluid-sensitive sequences in a tissue phantom study and with STIR, which is a most widely used conventional fluid-sensitive sequence, in a volunteer study for the assessment of postoperative cervical spine with ADR.

In the tissue phantom study, MAVRIC SL STIR was the best in the reduction of area of signal void, depiction of anatomy, and reduction of distortion and signal pile-up artifacts among variable fat-suppressed fluid-sensitive sequences. Our volunteer study also proves the increased visualization of anatomic detail by decreasing the area of signal void and distortion, as in our tissue phantom study and prior studies.[7] The spinal cord and neural foramina were almost clearly visualized in MAVRIC SL STIR with near absence of distortion in both tissue phantom and volunteer study. MAVRIC SL suppresses metal artifacts by combining multiple individual spectral bins acquired at different frequency offsets.[7,15,16] The MAVRIC SL approach is designed to address off-resonance artifacts that cause static magnetic field variations, resulting in signal loss, signal pileup, and distortion artifacts.[15,16] The most important effect of the MAVRIC SL technique was the reduction of the area of signal void that enabled us to better delineate the anatomy and detect pathologic tissue.[7,15] For example, MAVRIC SL STIR may visualize postoperative complication or infectious tissue that cause spinal cord and nerve root compression, such as prevertebral edema, hematoma, and abscess, which are not visible in STIR because of metallic artifact.

On the other hand, the image quality of the spinal cord of MAVRIC SL STIR images were degraded and determined to be clinically limited because of blurring. In our volunteer study, STIR showed better image quality than MAVRIC SL STIR with

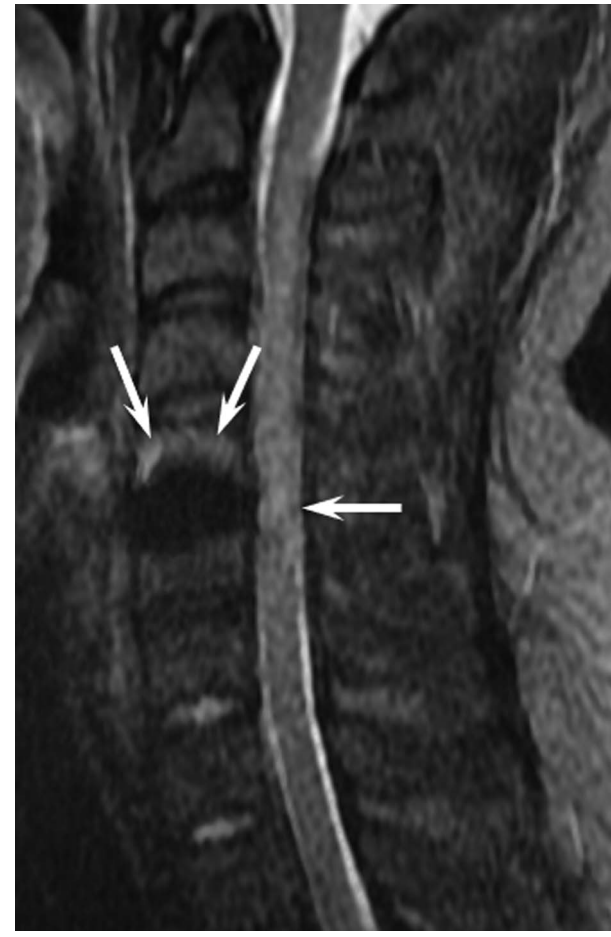

FIGURE 7. Midsagittal images of MAVRIC SL STIR of the cervical spine of a 32-year-old man with ADR at C5–C6 (volunteer 3). Ill-defined, mild high signal intensities (arrows) are seen at the C5 body and spinal cord adjacent to the operated site. This patient did not show any abnormal signal intensity in the C5 vertebral body and spinal cord in preoperative MRI and no clinical symptom. Therefore, these are not the true pathology but signal pile-up artifacts. Note the moderate blurring and noise in the spinal cord with limited clinical use.

statistical significance in the sagittal plane. MAVRIC SL used a longer ETL and 3-dimensional (3D) FSE acquisition that can result in increased blurring compared with 2-dimensional (2D) FSE.[15,16] This could be an important limitation for detailed evaluation of spinal cord signal change. In addition, the MAVRIC SL STIR showed ill-defined, weak high signal intensity of signal pile-up artifact around the metal in the volunteer study. Although the intensity and extent of the signal pile-up artifact may have much decreased, distinguishing true pathology becomes more difficult because of ill-defined, less intense characteristics; if present in the bone marrow or spinal cord, it could mimic bone marrow edema or myelopathy. Therefore, when a lesion in the spinal cord is clinically suspected, MAVRIC SL STIR should be used complementary to STIR for evaluation of the spinal cord signal change.

In terms of fat suppression, MAVRIC SL STIR was less homogeneous than STIR and Dixon techniques in the tissue phantom study. Although not statistically significant, even in a volunteer study, MAVRIC SL STIR showed slightly lesser homogeneous fat suppression than STIR. Kretzschmar et al[7] pointed out that the reduced fat saturation of MAVRIC SL STIR could have led to some false-negative diagnoses. Although the same principle of inversion recovery was adopted to suppress the fat signal in both 2D FSE-STIR and MAVRIC SL STIR, different radio frequency (RF) pulses were used in each sequence to implement the inversion recovery. In 2D FSE-STIR, a 180-degree slice-selective RF pulse was used for the inversion while, in MAVRIC SL STIR, a high-bandwidth adiabatic inversion pulse was used to match the 3.2-kHz bandwidth of the excitation RF pulse.[17] Another factor to note is that the intensive RF power deposition of MAVRIC SL forced lower flip angles for the all adopted RF pulses.[17] We suppose these differences of the RF pulse implementation and flip angle constraint in the MAVRIC SL STIR might cause the relatively lower fat suppression performance than other sequences.[17]

In our study, the scan time of MAVRIC SL STIR was more than 3 times longer than STIR in both axial and sagittal planes. MAVRIC SL uses a 3D encoding over the full FOV for each of up to 24 spectral bins and thus extending scan times compared with 2D-FSE techniques.[15,16] A long scan time is a major drawback of MAVRIC SL STIR, because patients with severe pain or in critical condition may fail to complete the MRI scan or have severe motion artifacts.

Our study has several limitations. First, there are various types of artificial disks, but only one type of artificial disk (Prodisc-C) was used in our study. Because of cobalt chrome keel of Prodisc-C, metallic artifact may be more severe than titanium components. However, even titanium artificial disks are known to have severe metallic artifacts.[5,17] This is related to the anteroposterior dimension of the artificial disk for the cover of the end plate, as we have previously mentioned. Therefore, although there is a difference in degree, our results may be applicable to other artificial disks. Second, because we used only one tissue phantom, statistical analysis cannot be performed in the tissue phantom study. Third, we aimed to compare images of MAVRIC SL STIR with variable fluid-sensitive sequences. However, we only compared MAVRIC SL STIR with STIR in the volunteer study because of scan time limitation. Because of difficulty in tolerating a prolonged scan time even for volunteers, we selected only STIR, which showed superior metal artifact reduction after MAVRIC SL STIR in the tissue phantom study. Fourth, the number of volunteers was small. In particular, axial scan was performed by only 3 volunteers, so statistically significant results were not obtained. Fifth, we did not perform a patient study with symptoms and pathology. Therefore, the diagnostic performance of pathology among sequences was not available. Expanding sample sizes and including patients will certainly contribute further to the evaluation. Sixth, we analyzed most of the artifacts qualitatively, except for the signal void area. Therefore, we performed independent analysis and calculated the interreader reproducibility for the reliability of the qualitative analysis.

In conclusion, MAVRIC SL STIR might be useful for visualization of anatomy by reduction of signal void areas and distortion in the operated site but should be used as a complement to STIR for evaluation of the spinal cord signal change.

ACKNOWLEDGMENTS

We extend special thanks to scientists and applicators in GE Healthcare, including Youngju Lee. We also deeply appreciate Myungpyo Hong for supplying the artificial disk instrument.

REFERENCES

1. Coric D, Nunley PD, Guyer RD, et al. Prospective, randomized, multicenter study of cervical arthroplasty: 269 patients from the Kineflex|C artificial disc investigational device exemption study with a minimum 2-year follow-up: clinical article. *J Neurosurg Spine*. 2011;15:348–358.
2. Sasso RC, Anderson PA, Riew KD, et al. Results of cervical arthroplasty compared with anterior discectomy and fusion: four-year clinical outcomes in a prospective, randomized controlled trial. *J Bone Joint Surg Am*. 2011;93:1684–1692.
3. Fallah A, Akl EA, Ebrahim S, et al. Anterior cervical discectomy with arthroplasty versus arthrodesis for single-level cervical spondylosis: a systematic review and meta-analysis. *PLoS One*. 2012;7:e43407.
4. Cho DY, Liau WR, Lee WY, et al. Preliminary experience using a polyetheretherketone (PEEK) cage in the treatment of cervical disc disease. *Neurosurgery*. 2002;51:1343–1349; discussion 1349–1350.
5. Sundseth J, Jacobsen EA, Kolstad F, et al. Magnetic resonance imaging evaluation after implantation of a titanium cervical disc prosthesis: a comparison of 1.5 and 3 Tesla magnet strength. *Eur Spine J*. 2013;22:2296–2302.
6. Sekhon LH, Duggal N, Lynch JJ, et al. Magnetic resonance imaging clarity of the Bryan, Prodisc-C, Prestige LP, and PCM cervical arthroplasty devices. *Spine (Phila Pa 1976)*. 2007;32:673–680.
7. Kretzschmar M, Nardo L, Han MM, et al. Metal artefact suppression at 3 T MRI: comparison of MAVRIC-SL with conventional fast spin echo sequences in patients with hip joint arthroplasty. *Eur Radiol*. 2015;25:2403–2411.
8. Lee YH, Lim D, Kim E, et al. Feasibility of fat-saturated T2-weighted magnetic resonance imaging with slice encoding for metal artifact correction (SEMAC) at 3T. *Magn Reson Imaging*. 2014;32:1001–1005.
9. Lee YH, Hahn S, Kim E, et al. Fat-suppressed MR imaging of the spine for metal artifact reduction at 3T: comparison of STIR and slice encoding for metal artifact correction fat-suppressed T_2-weighted images. *Magn Reson Med Sci*. 2016;15:371–378.
10. Talbot BS, Weinberg EP. MR imaging with metal-suppression sequences for evaluation of total joint arthroplasty. *Radiographics*. 2016;36:209–225.
11. Guerini H, Omoumi P, Guichoux F, et al. Fat suppression with Dixon techniques in musculoskeletal magnetic resonance imaging: a pictorial review. *Semin Musculoskelet Radiol*. 2015;19:335–347.
12. Hayter CL, Koff MF, Shah P, et al. MRI after arthroplasty: comparison of MAVRIC and conventional fast spin-echo techniques. *AJR Am J Roentgenol*. 2011;197:W405–W411.
13. Lu W, Pauly KB, Gold GE, et al. SEMAC: slice encoding for metal artifact correction in MRI. *Magn Reson Med*. 2009;62:66–76.
14. Koch KM, Brau AC, Chen W, et al. Imaging near metal with a MAVRIC-SEMAC hybrid. *Magn Reson Med*. 2011;65:71–82.
15. Choi SJ, Koch KM, Hargreaves BA, et al. Metal artifact reduction with MAVRIC SL at 3-T MRI in patients with hip arthroplasty. *AJR Am J Roentgenol*. 2015;204:140–147.
16. Gutierrez LB, Do BH, Gold GE, et al. MR imaging near metallic implants using MAVRIC SL: initial clinical experience at 3T. *Acad Radiol*. 2015;22:370–379.
17. Kaushik SSHA, LaViolette P, Nencka A, et al. Lipid suppression around metal implants using a B1-optimized adiabatic inversion pulse. *Proc Int Soc Magnet Resonance Med*. 2017;5028.